Nuclear Engineering and Design 445 (2025) 114515

Contents lists available at ScienceDirect

Nuclear Engineering and Design

journal homepage: www.elsevier.com/locate/nucengdes

PARCS pin-wise simulation with a cross section correction system based on the Super-Homogenisation method

Kanglong Zhang *, Luigi Mercatali, Victor Hugo Sanchez-Espinoza

Karlsruhe Institute of Technology (KIT), Hermann-von-Helmholtz-Platz 1, 76344 Eggenstein-Leopoldshafen, Germany

ARTICLE INFO

Keywords:
PARCS
Pin-wise
Cross-Section(XS)
Super-Homogenisation(SPH)
Serpent2

ABSTRACT

A cross-section (XS) correction system was developed at the Karlsruhe Institute of Technology (KIT) for pin-wise simulations in PARCS, utilizing the SuPer-Homogenization (SPH) method in an iterative Python-based framework. The system uses Monte Carlo Serpent2 pin-wise solutions as a reference to correct homogenized pin-wise XS, improving PARCS' accuracy in predicting neutron reaction rates and pin-wise power distributions. Verification was conducted with four test cases of increasing complexity: (a) a 3x3 mini assembly, (b) KONVOI reactor fuel assemblies, (c) a 3x3 mini-core, and (d) the Karlsruhe Small Modular Reactor (KSMR). Results show that the corrected XS significantly enhances PARCS' diffusion solver accuracy, closely matching Serpent2 results, in pin-by-pin core simulations. Notably, this approach outperforms traditional assembly-wise Pin Power Reconstruction (PPR), particularly in central core regions. The key outcome of this work is that, for PARCS pin-wise simulations, computational accuracy is enhanced, making the prediction of local safety parameters feasible, especially if coupled with a Thermal-Hydraulic (TH) code, such as a sub-channel code. Furthermore, this work extends PARCS's capability to perform pin-wise simulations with the standard nodal solver.

1. Introduction

The prediction of local safety parameters within the reactor core is crucial for nuclear safety analysis, requiring pin-wise solutions for both neutronic and Thermal-Hydraulic (TH) fields, which are generated by specialized computational tools. Sub-channel codes are typically used for pin-level core TH. As to pin-level neutronics, deterministic transport and Monte Carlo (MC)codes are widely employed. These neutronic codes utilize advanced algorithms and methods that enable highly detailed and accurate simulations, consequently requiring significant computational resources.

In contrast, deterministic codes, which solve the neutron diffusion or simplified transport equation (such as SP3), are much faster. This speed is partly because deterministic codes are usually designed for assembly-wise simulations with smaller problem scales and nodal solvers. Even when applied to pin-level simulations, deterministic codes are more efficient, but they tend to be less accurate. To balance speed, accuracy, and pin-wise resolution, diffusion deterministic codes often use nodal solvers for assembly-wise simulations and reconstruct the pin-wise fields through the Pin Power Reconstruction (PPR) method. This approach offers the advantage of faster computations and reasonable pin-power predictions, however, it is not a true pin-wise solution and does not allow local pin-wise TH feedback to be accommodated, limiting its accuracy in pin-level multi-physics simulations.

Therefore, accurate core simulations at the pin level, using real condensed and homogenized pin-wise cross sections (XS), are necessary. However, such simulations can be prone to errors, primarily due to pin-wise homogenization errors. To address that, the pin-wise XS are usually corrected to let the diffusion or quasi-diffusion codes be able to: 1) reserve the reaction rate in the cell; 2) keep the neutron flux continuity at the cell boundaries; 3) reflect the neutron heterogeneous leakage, with the high-fidelity resolutions. Representative correction methods include Generalized Equivalence Theory (GET) (Smith, 1986); Super-Homogenization (SPH) factor (Kavenoky, 1980), Eddington factor, and the Albedo-corrected Parameterized Equivalence Constants (APEC) methods (Kim et al., 2017), benefit from which, practical full-core pin-wise diffusion simulations are achievable. The most recent such work can be found in (Kim and Kim, 2019, 2020; Wang et al., 2025; Zhang et al., 2024; Zhuang et al., 2024). It is to noting that, among those methods, the standard SPH is a "hanging" method and could be used for "black-box" traditional two-step neutronic calculations, which is our condition using Serpent and PARCS. So, the SPH method was selected in

* Corresponding author.
E-mail addresses: kanglong.zhang2@kit.edu (K. Zhang), luigi.mercatali@kit.edu (L. Mercatali), victor.sanchez@kit.edu (V.H. Sanchez-Espinoza).

https://doi.org/10.1016/j.nucengdes.2025.114515
Received 3 July 2025; Received in revised form 29 September 2025; Accepted 2 October 2025
Available online 8 October 2025

this paper. Moreover, to clearly demonstrate the SPH functionality, no other methods, e.g., discontinuity factor, are adopted.

The SPH method, first proposed by Kavenoky in 1978 (Kavenoky, 1980); was developed to correct pin-wise homogenized XS for transport codes. Over the years, extensive work by Hébert (Hébert and Kavenoky, 1981; Hébert and Benoist, 1991; Hebert, 1993; Hebert and Mathonniere, 1993) has refined the SPH algorithm, which is now considered mature and standardized (Hebert and Mathonniere, 1993). The SPH method generates homogenized XS for transport codes based on heterogeneous solutions, ensuring the preservation of reaction rates. Recent advancements have improved the SPH performance, including flux discontinuity correction between assemblies (Yamamoto et al., 2004) and the variant PJFNK-SPH method (Preconditioned Jacobian-Free Newton–Krylov) (Laboure et al., 2019; Ortensi et al., 2018). The SPH method continues to attract attention and has been applied across various codes and conditions (Grundmann and Mittag, 2011; Sen et al., 2017; Yuan et al., 2022); with recent applications combining it with multi-physics systems for more reliable simulations (Li et al., 2023).

At the Karlsruhe Institute of Technology (KIT), ongoing research and development efforts aim to create computational schemes capable of analyzing local safety parameters at the pin level by coupling the PARCS (Downar et al., 2012) core neutronic code with sub-channel TH solvers. For this to be feasible, PARCS must accurately simulate the entire reactor core at the pin level. To achieve this, two key developments were made: (a) PARCS was further enhanced at KIT to enable pin-wise simulations with standard nodal solvers, and (b) an SPH-based pin-wise XS correction system was developed. In this approach, XS is generated using the Serpent2 code (Leppänen et al., 2015). The key concept of the SPH-based scheme is to correct Serpent2 pin-wise XS by ensuring that the neutron reaction rates in PARCS match those from Serpent2.

It is worth noting that Serpent2 is employed in this study for XS generation because it is actively used in our group. The proposed SPH-based correction framework is not restricted to Serpent2. In principle, the methodology can be applied with any lattice or transport code capable of providing homogenized pin-wise cross sections, including deterministic codes such as CASMO and HELIOS.

2. The functional extension for PARCS

2.1. Basics of PARCS

It should be noted that the PARCS we use in this paper is V331. Here below, if not specified, PARCS refers to PARCS V331. PARCS is a three-dimensional (3D) reactor core code that solves steady-state and time-dependent multi-group neutron diffusion or low-order neutron transport equations for Cartesian and hexagonal fuel geometries. Developed by the U.S. Nuclear Regulatory Commission (NRC), its primary purpose is to provide an approximate yet accurate numerical model of the physical reactor system. Typically, PARCS employs the Nodal Expansion Method (NEM) to perform two-node solutions at the assembly level, while the PPR method is used for pin-level prediction, such as fuel pin power, which is crucial for detailed core safety assessments.

For reactor kinetics calculations, PARCS requires both the geometry and the multi-group XS as input. These XS are typically generated by Monte Carlo (MC) codes, such as Serpent2 in this work, and stored in PMAXS files. These files serve as the interface between the XS generation by MC codes and PARCS, providing all necessary XS data for both steady-state and transient calculations. The data include macroscopic XS, microscopic XS for xenon and samarium, group-wise form functions for various branch states (as a function of temperature, density, burnup, etc.), and kinetic parameters. GENPMAXS is the standard tool used by PARCS to generate PMAXS files (Ward et al., 2016) requiring a GenPMAXS text file as the input.

While Serpent2 is used in the present work to supply the XS data, other codes such as CASMO, HELIOS, or DRAGON can also generate the PMAXS interface for PARCS. The SPH-based correction system developed here is independent of the XS source and could be readily applied in combination with these codes.

2.2. PARCS for pin-wise simulation

PARCS offers two approaches for generating pin-wise fields:

1) Nodal solver + PPR. This method runs quickly but is not designed for true pin-level simulations.
2) Fine Mesh Finite Difference (FMFD) kernel. This approach uses an SP3 solver capable of real pin-level simulations. However, the fuel rod is not explicitly defined, as the hierarchy moves from rod to assembly to core, which introduces challenges for achieving pin-level thermal–hydraulic (TH) feedback due to the "assembly" layer encapsulating the fuel rods.

Since true pin-level simulations with explicit fuel rod definitions are required to enable pin-level TH feedback, neither of these approaches is fully adequate. Therefore, we extended PARCS's capability by utilizing normal NEM or ANM solvers, instead of the FMFD kernel, to benefit from explicit pin definitions. However, it was discovered that PARCS, with standard nodal solvers like NEM or ANM, could not handle large-scale problems (e.g., 200x200-sized cases).

The limitations were identified in the input and output processing, presenting as a "capacity" or "data traffic" issue. This problem was resolved by modifying the PARCS source code, enabling the KIT variant of PARCS V331 to process large datasets using normal nodal solvers. This advancement opens the door for applying the SPH system to full-core analyses.

3. The SPH-based pin-wise XS correction system

The SPH method is an iterative technique that applies a set of SPH factors to correct the XS for each equivalence region and energy group in deterministic codes. For instance, if a model contains 9 pins and 2 energy groups, there would be 18 SPH factors. Within this framework, Serpent2 runs once to generate reference results, typically at the assembly level with pin-wise resolution. PARCS then runs iteratively to approximate Serpent2 results, such as neutron reaction rates at the pin level. During each iteration, after a step is completed, the SPH factors for the next step are calculated based on the current PARCS flux and the reference Serpent2 flux. The XS for each region and energy group in PARCS are updated by multiplying these factors. The iteration continues until the differences in neutron reaction rates between PARCS and Serpent2 fall within a specified criterion.

The working principle of the SPH-based XS correction system in this study is outlined below. For simplicity, the model is assumed to contain only one cell and one energy group, and the various XS adopted by different codes are simplified as total/fission/leakage XS.

1) Serpent2 runs a computation at the fuel assembly level and produces pin-wise heterogeneous results at criticality mode.
   - $A_{tot-R}^{Serpent}$ – total neutron reaction rate, including absorption, fission, etc.
   - $A_{tot-F}^{Serpent}$ – total fission rate.
   - $A_{tot-L}^{Serpent}$ – total leakage rate.
   - $\phi_{tot}^{Serpent}$ – total neutron flux.
2) The system computes the pin-wise homogenized XS based on Serpent2 results.
   - $\Sigma_R^{Homo} = \frac{A_{tot-R}^{Serpent}}{\phi_{tot}^{Serpent}}$ – the homogenized total XS.
   - $D_L^{Homo} = \frac{A_{tot-L}^{Serpent}}{B^2 \phi_{tot}^{Serpent}}$ – the homogenized diffusion coefficient, which has reciprocal relations with the macro transport XS, where B is the buckling.
   - $\Sigma_F^{Homo} = \frac{A_{tot-F}^{Serpent}}{\phi_{tot}^{Serpent}}$ – the homogenized fission XS.

3) The system introduces those homogenized XS to PARCS, do the computation, get the pin-wise neutron flux ϕ_{tot}^{Parcs}. Due to the solution difference between PARCS and Serpent2, ϕ_{tot}^{Parcs} normally not equal $\phi_{tot}^{Serpent}$. So that we know:

- $\Sigma_R^{Homo} \bullet \phi_{tot}^{Parcs} \neq \Sigma_R^{Homo} \bullet \phi_{tot}^{Serpent} = A_{tot-R}^{Serpent}$
- $D_L^{Homo} \bullet \phi_{tot}^{Parcs} \neq D_L^{Homo} \bullet \phi_{tot}^{Serpent} = A_{tot-L}^{Serpent}$
- $\Sigma_F^{Homo} \bullet \phi_{tot}^{Parcs} \neq \Sigma_F^{Homo} \bullet \phi_{tot}^{Serpent} = A_{tot-F}^{Serpent}$

To preserve the pin-wise rates between PARCS and Serpent2, the system multiplies a so-called SPH factor μ^0 to the PARCS solution, as fpllows:

- $\Sigma_R^{Homo} \bullet \phi_{tot}^{Parcs} \bullet \mu^0 = \Sigma_R^{Homo} \bullet \phi_{tot}^{Serpent} = A_{tot-R}^{Serpent}$
- $D_L^{Homo} \bullet \phi_{tot}^{Parcs} \bullet \mu^0 = D_L^{Homo} \bullet \phi_{tot}^{Serpent} = A_{tot-L}^{Serpent}$
- $\Sigma_F^{Homo} \bullet \phi_{tot}^{Parcs} \bullet \mu^0 = \Sigma_F^{Homo} \bullet \phi_{tot}^{Serpent} = A_{tot-F}^{Serpent}$

4) The factor μ is calculated via $\mu^0 = \frac{\phi_{tot}^{Serpent}}{\phi_{tot}^{Parcs}}$. To introduce this correction to the PARCS solution, the system multiplies this SPH factor to the homogenized XS of PARCS. The updated XS now becomes:

- $\Sigma_{R,\ new}^{Homo} = \Sigma_R^{Homo} \bullet \mu^0$– the updated homogenized total XS.
- $D_{L,\ new}^{Homo} = D_L^{Homo} \bullet \mu^0$– the updated homogenized diffusion coefficient, which has reciprocal relations with the macro transport XS, where B is the buckling.
- $\Sigma_{F,\ new}^{Homo} = \Sigma_F^{Homo} \bullet \mu^0$- the updated homogenized fission XS.

5) With the updated XS, PARCS runs a new calculation getting the new neutron flux, based on which the new SPH factor could be calculated. With the new SPH factors, PARCS will update its XS again and run a new calculation.
6) Such procedure is iterated until the difference between the new SPH factor and the previous one meets a defined convergence criterion, providing in this way the indication that the fluxes computed by PARCS preserve the ones computed by Serpent2.

It is important to note that SPH factors are not directly calculated using neutron fluxes but rather with normalized neutron fluxes. This normalization aims to eliminate discrepancies in flux levels between different codes. However, Yamamoto observed that this normalization does not perform well in multi-assembly calculations where different assembly types are adjacent. The conventional normalization method does not account for flux discontinuities between assemblies, which increases homogenization errors in the peripheral regions of assemblies. To address this issue, Yamamoto developed an improved SPH method, where SPH factors are divided by an averaged “cell-level” discontinuity factor obtained from each fuel assembly (Yamamoto et al., 2004). Despite its potential, this method has yet to gain widespread validation or use.

Generally, the standard SPH method suffices for most cases. Grundmann implemented the SPH method in the neutronics code DYN3D (Grundmann and Mittag, 2011); while Lemarchand applied it to pin-by-pin calculations using the code QUABOX/CUBBOX (Lemarchand et al., xxxx). Nikitin uses this method in nodal diffusion analysis of Sodium Fast Reactor (SFR) cores (Nikitin et al., 2015). and Sen applied it to High-Temperature Reactors (HTRs) (Sen et al., 2017); In this document, we also employ the standard SPH method.

All system components are coordinated by Python. The steps of the SPH procedure, assuming the PARCS model has 9 cells/pins, are as follows:

1) The Serpent2 executable reads its input file and runs, producing output files.
2) The system processes the Serpent2 output files containing XS data to generate 9 files as inputs for GenPMAXS.
3) The system generates 9 standard input files for GenPMAXS.
4) GenPMAXS is launched 9 times (once for each cell), producing 9 PMAXS files, which are read by PARCS as XS input files.
5) PARCS reads its input and XS files and produces output files containing neutron flux, power, and Keff. This step repeats until the normalized PARCS pin-wise power matches that of Serpent2. In each iteration, 9 SPH factors are calculated to correct the XS data. Relevant data during the SPH process are recorded in DATA files.
6) Python scripts parse the DATA files for post-processing.

4. Verification of the XS correction system

The computational procedure described above has been verified using four test cases with increasing complexity, as follows:

1) a 3x3 mini academic assembly.
2) nine typical fuel assemblies (16x16 pin arrangement) of the German KONVOI reactor.
3) a 3x3 mini core assembled by selected KONVOI fuel assemblies.
4) the core of an academic Small Modular Reactor (SMR) named KSMR (Karlsruhe SMR) developed at KIT.

For each case, three calculations have been performed, and their data sets have been compared:

1) Serpent2 solution as the reference.
2) PARCS solution without SPH – pin-wise XS.
3) PARCS solution with SPH – pin-wise XS.

Especially, for cases 3 and 4, the traditional PARCS solutions at the assembly level with PPR have also been included in the comparison. It should be noted that all cases presented in this study are based on fresh fuels. Nevertheless, the methodology is not restricted to unburned conditions. Since fuel burnup leads to changes in isotopic composition and thus in the underlying cross sections, separate XS libraries are typically prepared for different burnup states. The SPH correction procedure can then be applied independently to each burnup-dependent XS set, ensuring consistency across the entire depletion range. This extension is straightforward and will be addressed in future work.

4.1. The 3x3 mini academic assembly

The Sepent model and the geometrical dimensions of this assembly are given in Fig. 1.

On this model, a Serpent2 steady state criticality calculation has been performed with fully reflective boundary conditions. Neutron energy is divided into thermal and fast groups. The Serpent2 results are used as a reference for evaluating the subsequent PARCS simulations that have been performed for this case using pin-wise XS both without and with the SPH correction. The resulting Keff values are presented in Table 1.

With SPH, the Keff difference between PARCS and Serpent2 significantly decreases from 1.2e to 03 (without SPH) to 1.0e-05. This marked agreement demonstrates the positive impact of the SPH correction on the Keff prediction in PARCS. Besides Keff, the normalized pin power distribution is another very important parameter to be considered. Fig. 2 presents the relevant results, with the normalized power distribution of Serpent2 (top left) serving as the reference. The results from PARCS without SPH (top middle) deviate noticeably from the reference, while those with SPH (top right) closely match it. The difference is further highlighted in the bottom two plots: the maximum deviation with SPH is as low as 0.0261 %, compared to 0.351 % without SPH (calculated as abs (PARCS-Serpent2)/Serpent2). Thus, SPH has a significant positive effect on predicting pin power.

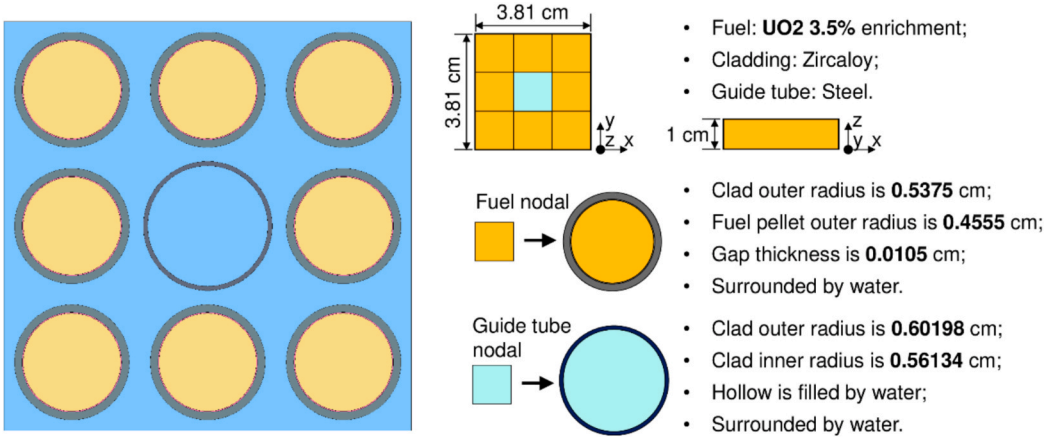

Fig. 1. The Serpent2 model (left) and the geometrical dimension (right) of the 3x3 mini assembly.

Table 1
The Keff results of the 3x3 mini assembly.

	SERPENT2	PARCS no SPH	PARCS on SPH
Keff	1.30203	1.30323	1.30204
K-Diff (PARCS-Serpent2)*10E5		120	1

4.2. The assemblies of the German KONVOI reactor

Nine typical KONVOI-type fuel assemblies are simulated in this case. The general configuration and geometrical dimensions of one of the assemblies are provided in Fig. 3.

It is important to note that the models being simulated do not represent real KONVOI assemblies, as the axial length of the models is only 1 cm. This adjustment is made to reduce the computational scale. Various configurations are modeled for the assemblies. For instance, the purple cell in the figure could represent a control rod or guide tube, while the yellow cell could correspond to a boron rod or guide tube. A total of nine subcases are simulated, as listed in Table 2.

Only steady-state calculations are performed, and all six surfaces use reflective boundary conditions. The neutron energy is divided into thermal and fast groups. The Keff results are presented in Table 3. With the application of SPH, the Keff differences between PARCS and Serpent2 decrease significantly compared to those without SPH, demonstrating a substantial correction and confirming the positive effect of SPH on Keff prediction in PARCS.

Figs. 4–12 illustrate the normalized pin power distributions for the

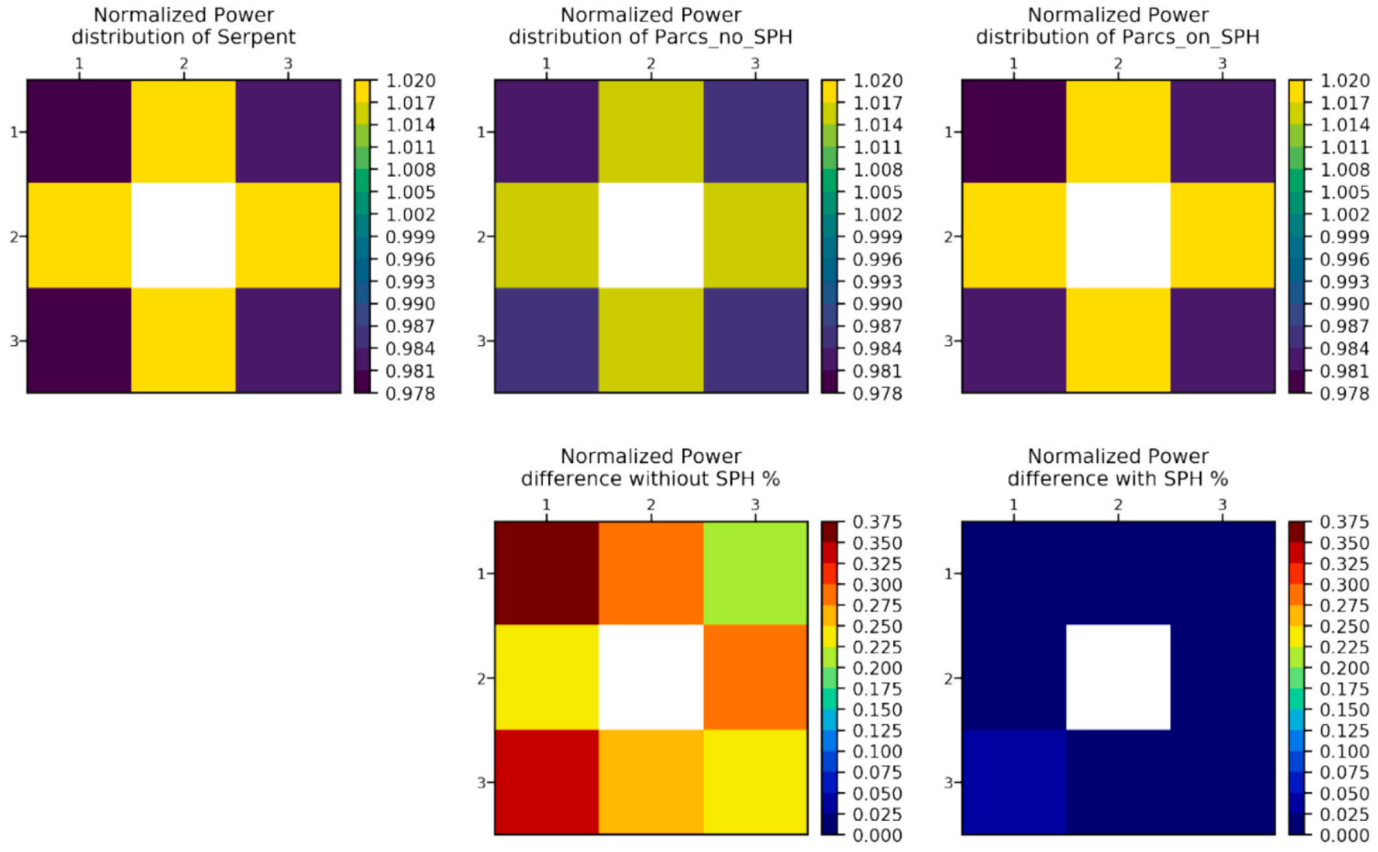

Fig. 2. The normalized pin power distribution of the 3x3 mini assembly.

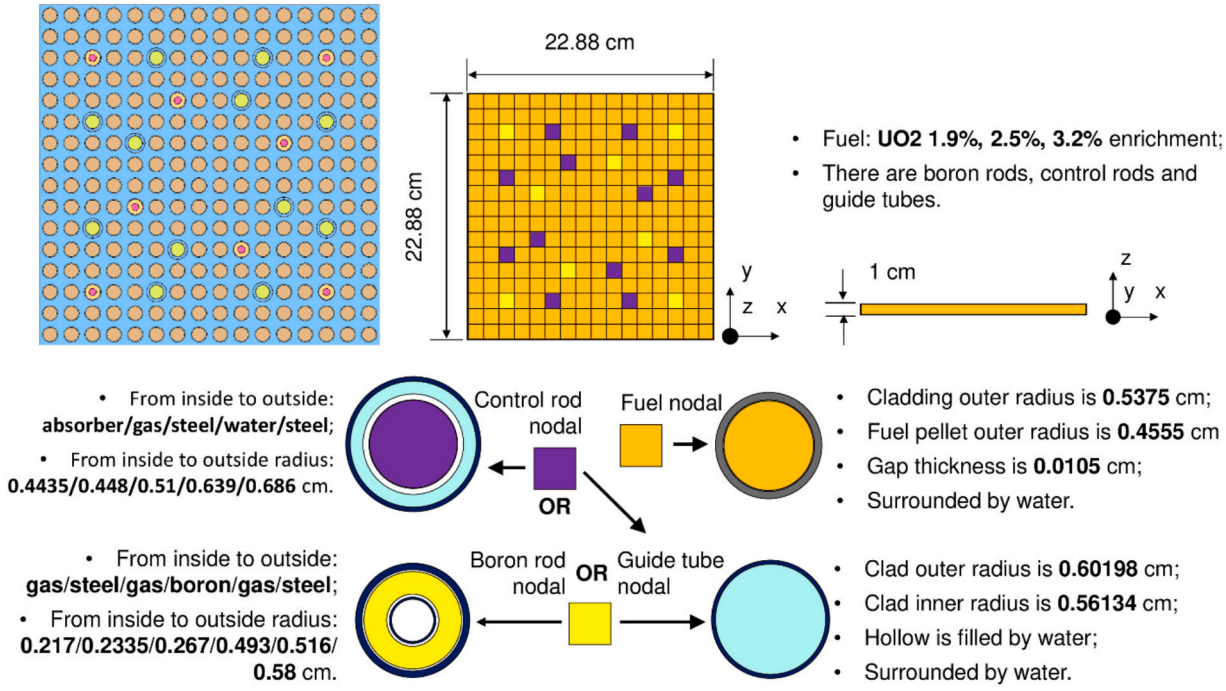

Fig. 3. The Serpent2 model (top left) and the geometrical dimension of one KONVOI type assembly.

Table 2
The subcases of KONVOI type assemblies.

Enrichment	1.9 %	2.5 %	3.2 %	
no boron, no control	subcase 1	subcase 2	subcase 3	purple – guide tube, yellow – guide tube
on boron, no control	subcase 4	subcase 5	subcase 6	purple – guide tube, yellow – boron rod
on boron, on control	subcase 7	subcase 8	subcase 9	purple – control rod, yellow – boron rod

Table 3
The Keff results of the KONVOI type assemblies.

		SERPENT2	PARCS no SPH	PARCS on SPH
subcase 1	Keff	1.20985	1.21073	1.20989
	K-Diff (PARCS-Serpent2)*10E5		88	4
subcase 2	Keff	1.28693	1.28788	1.28699
	K-Diff (PARCS-Serpent2)*10E5		95	6
subcase 3	Keff	1.34656	1.34750	1.34657
	K-Diff (PARCS-Serpent2)*10E5		94	1
subcase 4	Keff	1.10227	1.09861	1.10222
	K-Diff (PARCS-Serpent2)*10E5		−336	−5
subcase 5	Keff	1.18717	1.18422	1.18717
	K-Diff (PARCS-Serpent2)*10E5		−295	0
subcase 6	Keff	1.25471	1.25237	1.25464
	K-Diff (PARCS-Serpent2)*10E5		−234	−7
subcase 7	Keff	0.87334	0.85728	0.87318
	K-Diff (PARCS-Serpent2)*10E5		−1606	−16
subcase 8	Keff	0.95991	0.94488	0.95966
	K-Diff (PARCS-Serpent2)*10E5		−1503	−25
subcase 9	Keff	1.03347	1.19702	1.03317
	K-Diff (PARCS-Serpent2)*10E5		−1375	−30

nine subcases. In these figures, the normalized power distribution of Serpent2 (top left) serves as the reference. The results from PARCS without SPH (top middle) show noticeable deviations, whereas the results from PARCS with SPH (top right) closely match the reference. The differences are further highlighted in the bottom two plots, which display the relative differences (abs(PARCS-Serpent2)/Serpent2).

The maximum differences between the cases with SPH and those without SPH are summarized in Table 4. It is evident from these results that the application of the SPH methodology substantially increases the accuracy of the pin power prediction.

4.3. The 3x3 mini core

In this case, the mini core consists of 9 assemblies, arranged as shown in Fig. 13. The outer 8 assemblies correspond to subcase 1 from Section 4.2, with no boron or control rods, and an enrichment of 1.9 %. The central assembly corresponds to subcase 7, where both boron rods and control rods are inserted, also with an enrichment of 1.9 %.

Unlike the standard SPH calculation system outlined in Chapter 3, no iteration is performed in this case, and PARCS runs only once. The SPH factors for the two assembly types (1 and 7) are directly taken from the converged factors calculated in Section 4.2. Additionally, PARCS performs three calculations: one with SPH and pin-wise XS, one without SPH but with pin-wise XS, and a traditional nodal assembly-wise calculation with pin-power reconstruction.

As shown in Table 5, PARCS with pin-wise XS and SPH provide the best prediction of the mini core's Keff, while PARCS without SPH performs worse, and the traditional assembly-wise XS with PPR yields the poorest result.

Fig. 14 illustrates the pin power distributions for this case. The top left 1 plot shows the normalized power distribution from Serpent2, serving as the reference. The traditional PARCS solution is displayed in top left 2, PARCS without SPH is shown in top right 2, and PARCS with SPH is presented in top right 1. While the results look somewhat similar, the differences become more evident in the bottom plots. In the outer 8 assemblies, the differences between the three calculations are minor. However, in the central assembly, PARCS without SPH shows a significant discrepancy. The traditional PARCS solution results in smaller differences in the central assembly, but the differences at the boundaries, especially in the four corners, remain noticeable. PARCS with SPH performs the best, showing smaller discrepancies not only in the central assembly but also at its boundaries and corners.

The maximum difference with SPH is as low as 4.82e-02, while that without SPH is 9.31e-02, and the traditional PARCS solution is 7.38e-02 (abs(PARCS-Serpent2)/Serpent2). We can conclude that SPH has a

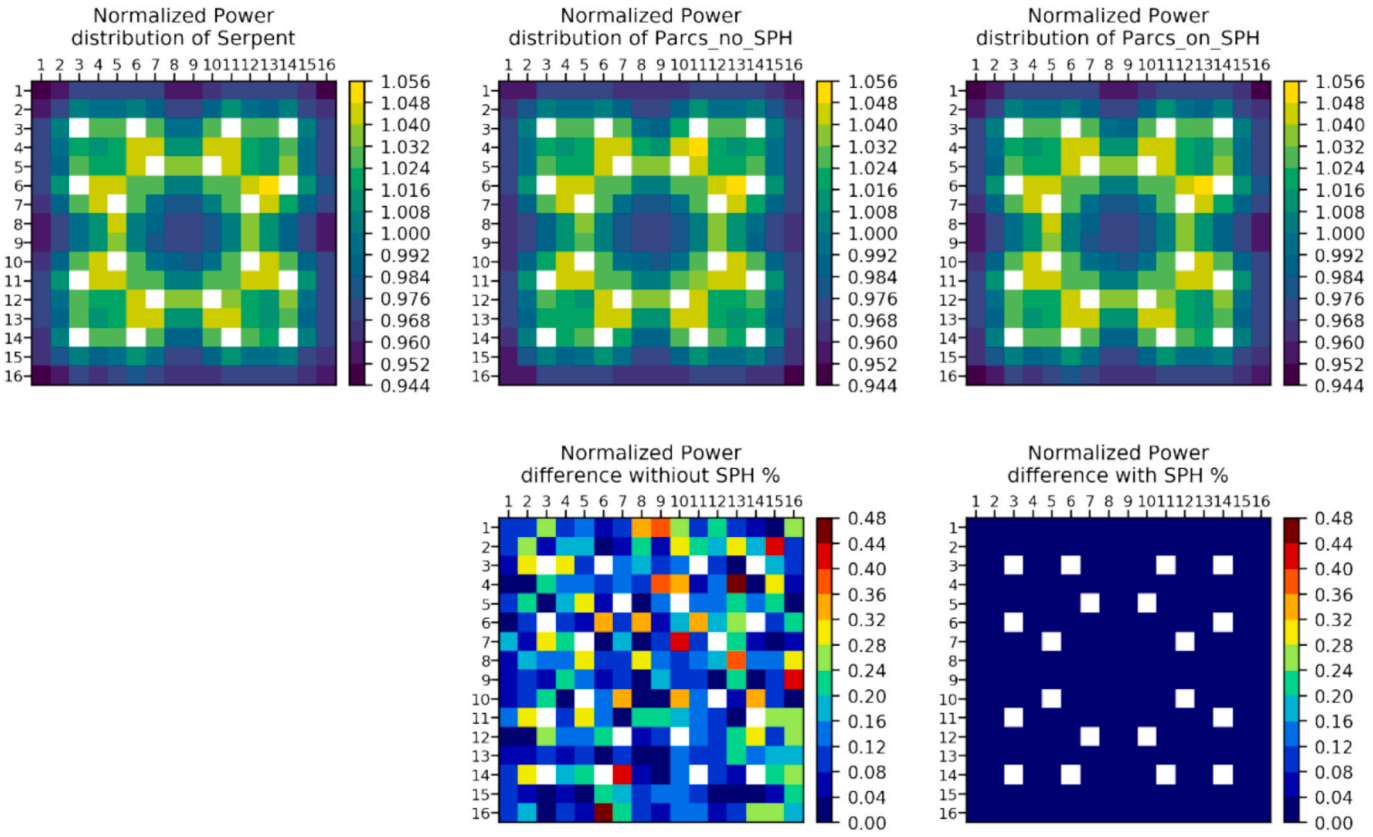

Fig. 4. The normalized pin power distribution of the KONVOI type assembly subcase 1.

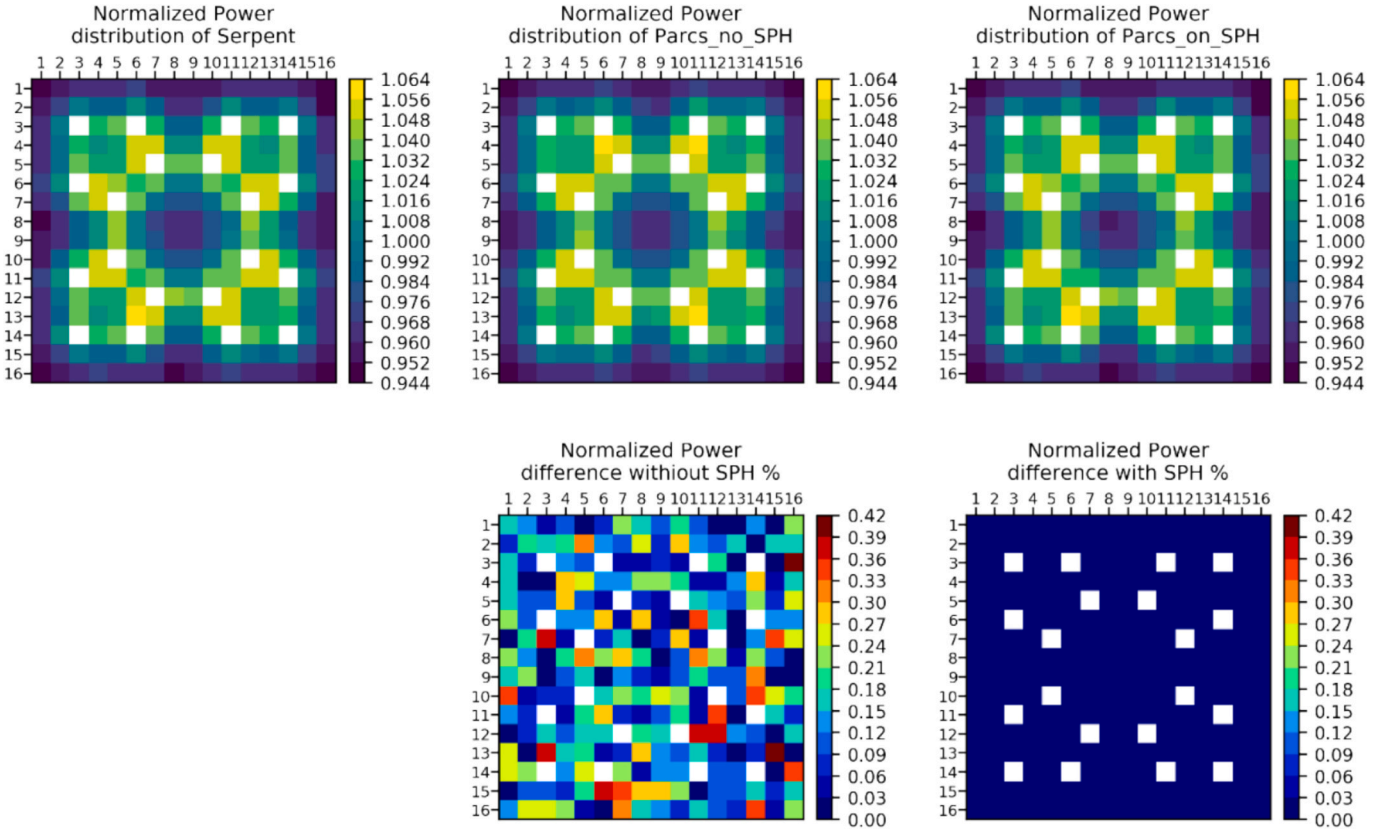

Fig. 5. The normalized pin power distribution of the KONVOI type assembly subcase 2.

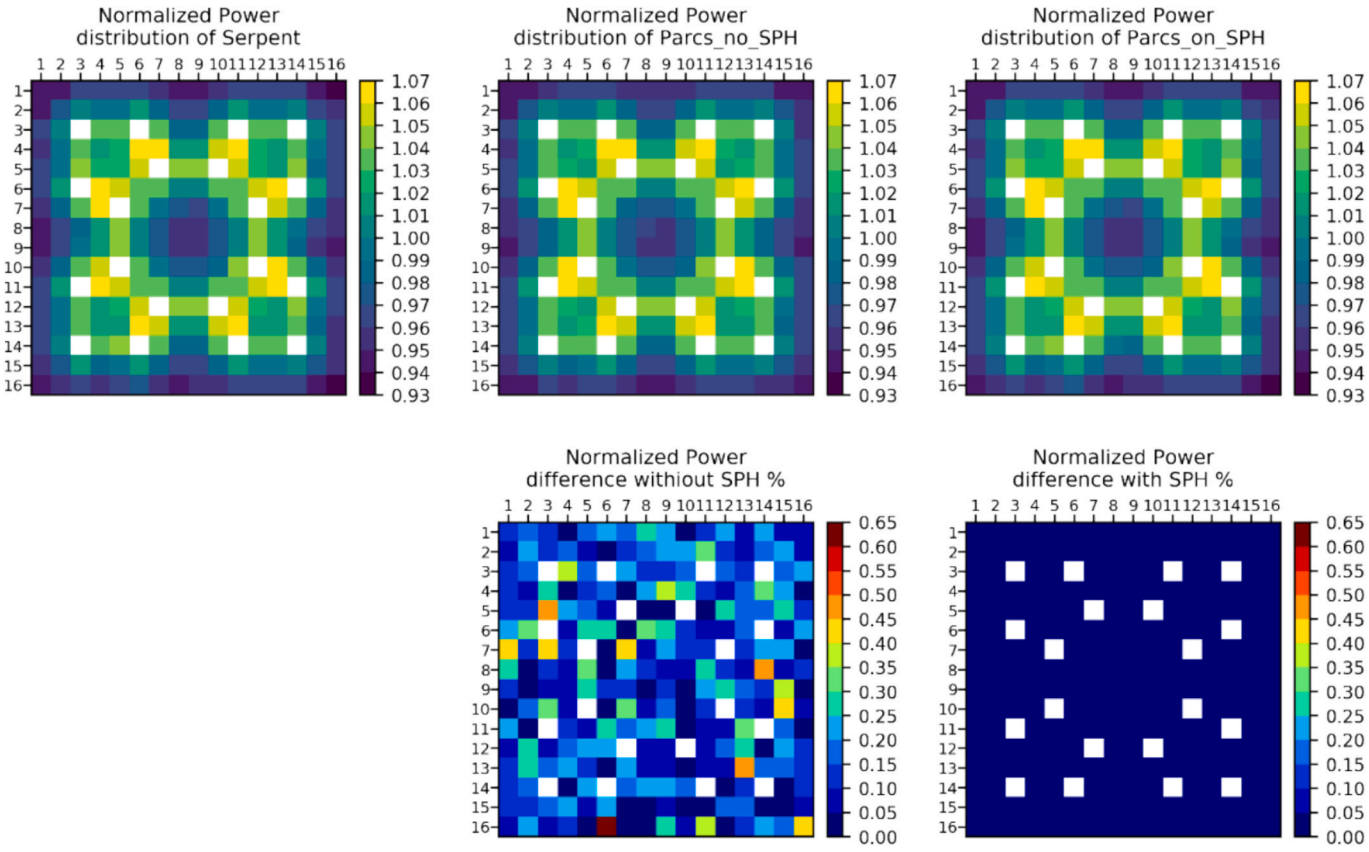

Fig. 6. The normalized pin power distribution of the KONVOI type assembly subcase 3.

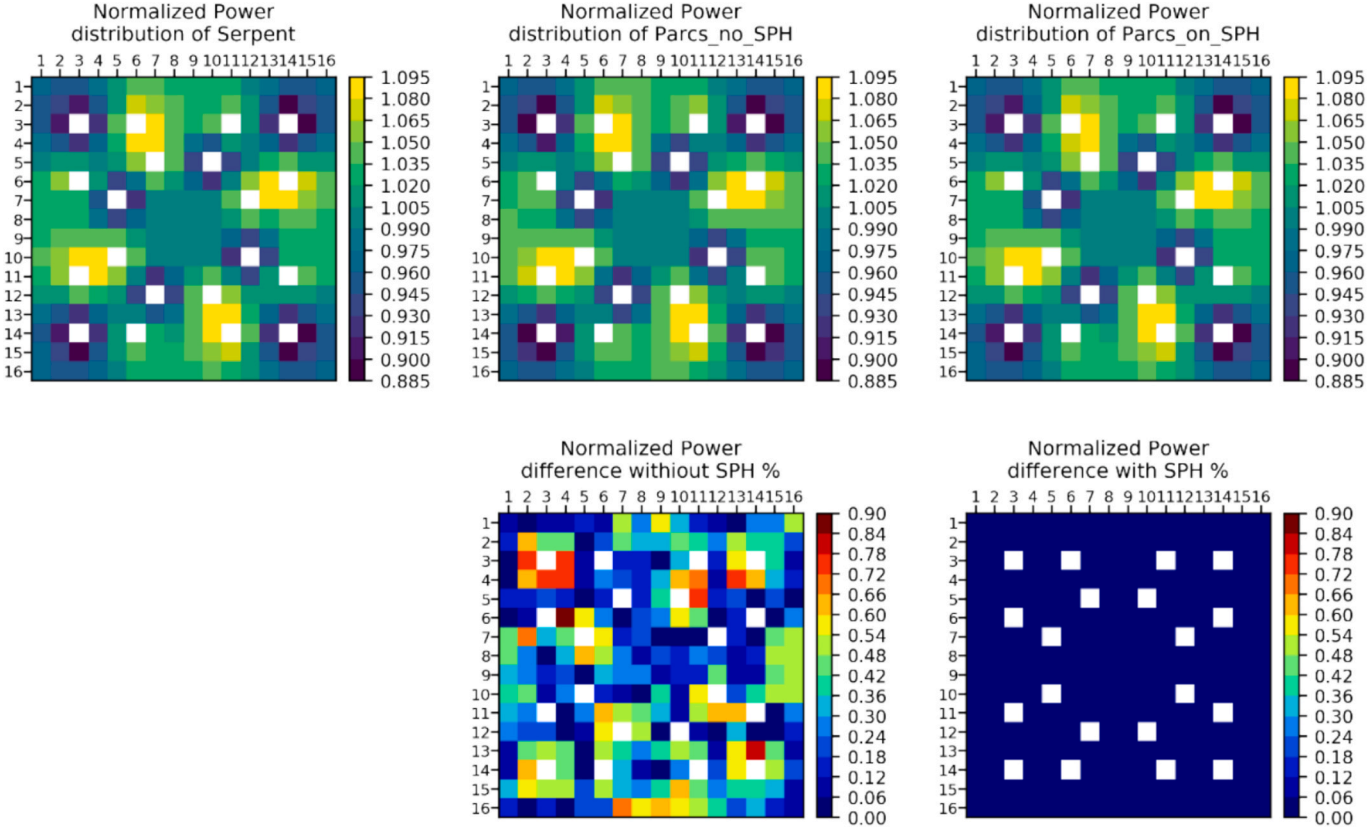

Fig. 7. The normalized pin power distribution of the KONVOI type assembly subcase 4.

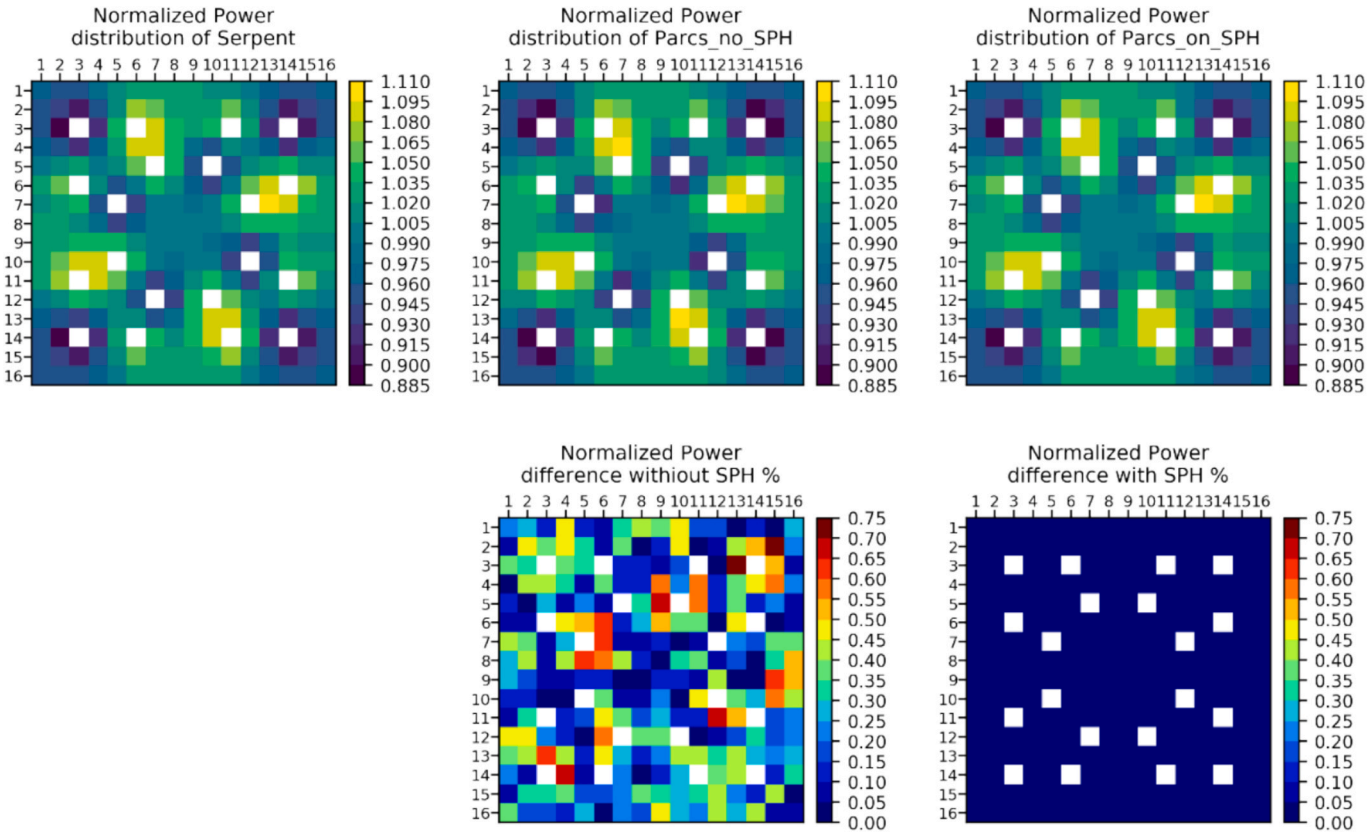

Fig. 8. The normalized pin power distribution of the KONVOI type assembly subcase 5.

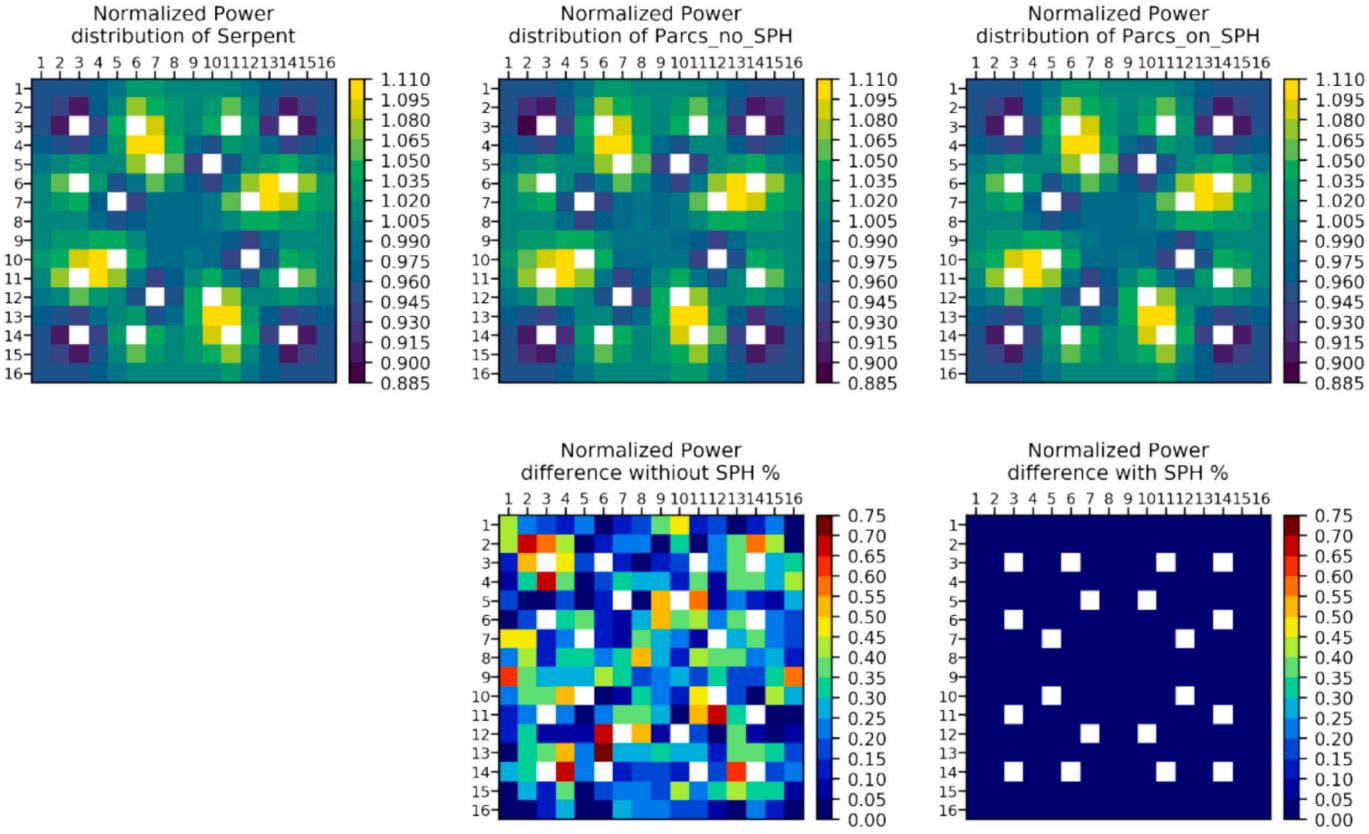

Fig. 9. The normalized pin power distribution of the KONVOI type assembly subcase 6.

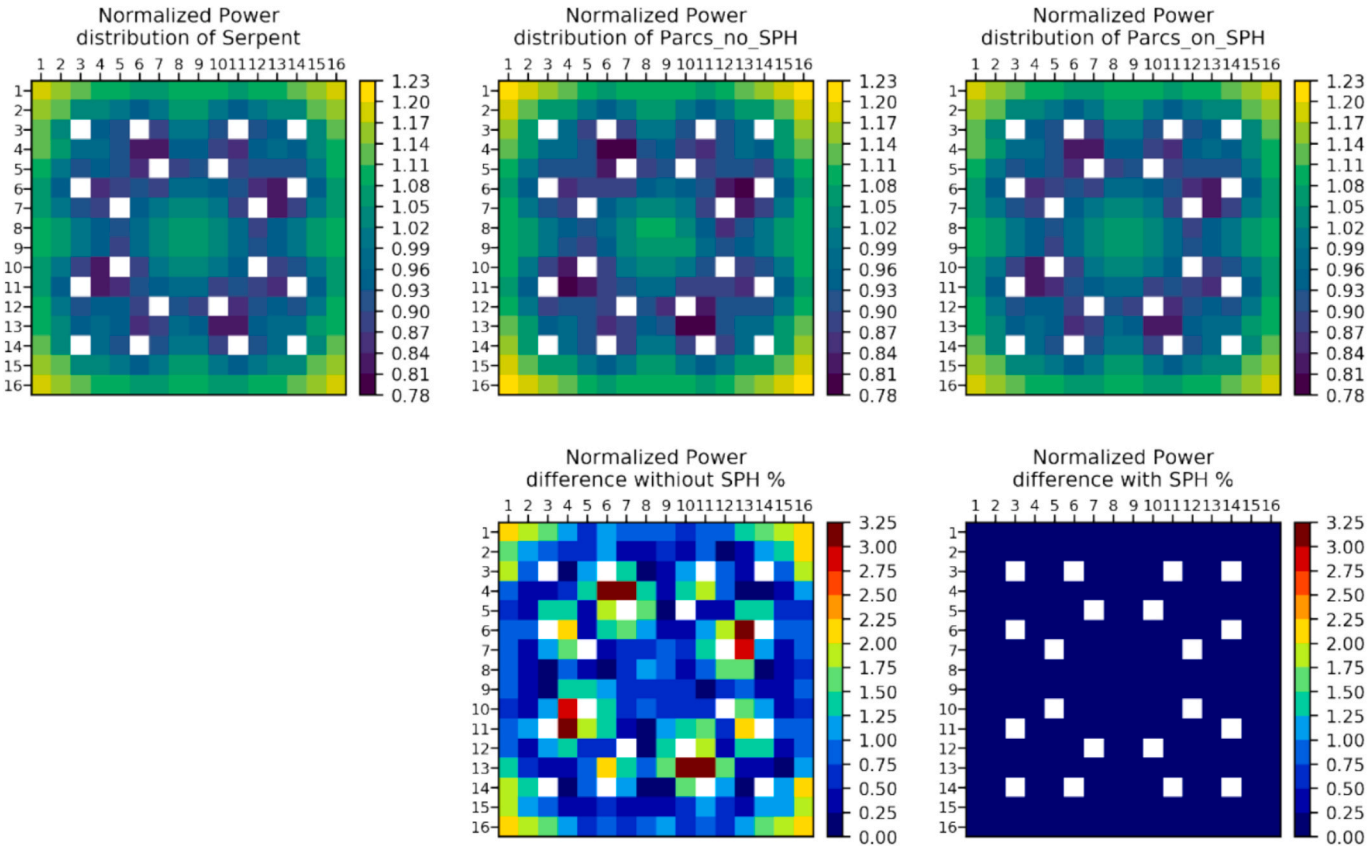

Fig. 10. The normalized pin power distribution of the KONVOI type assembly subcase 7.

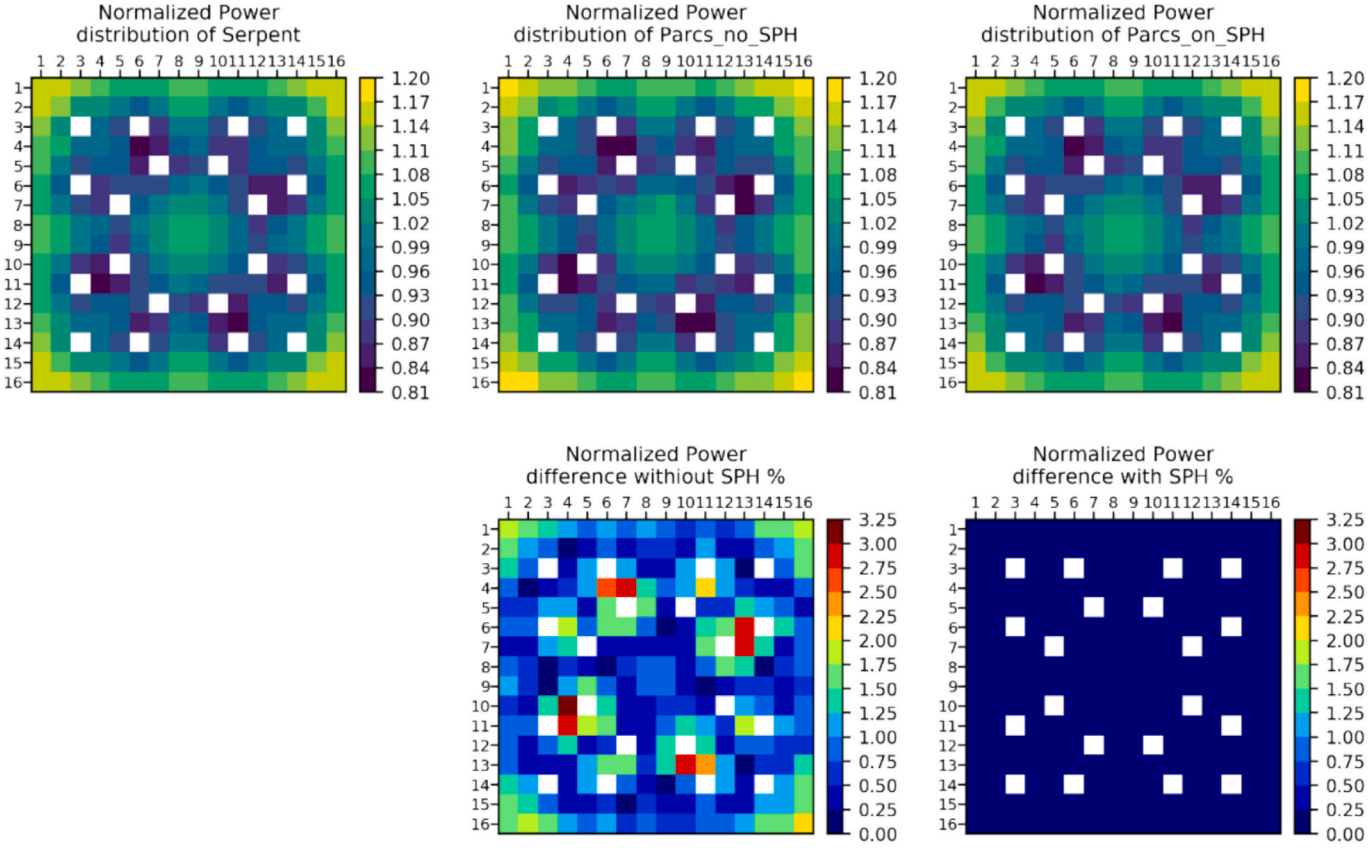

Fig. 11. The normalized pin power distribution of the KONVOI type assembly subcase 8.

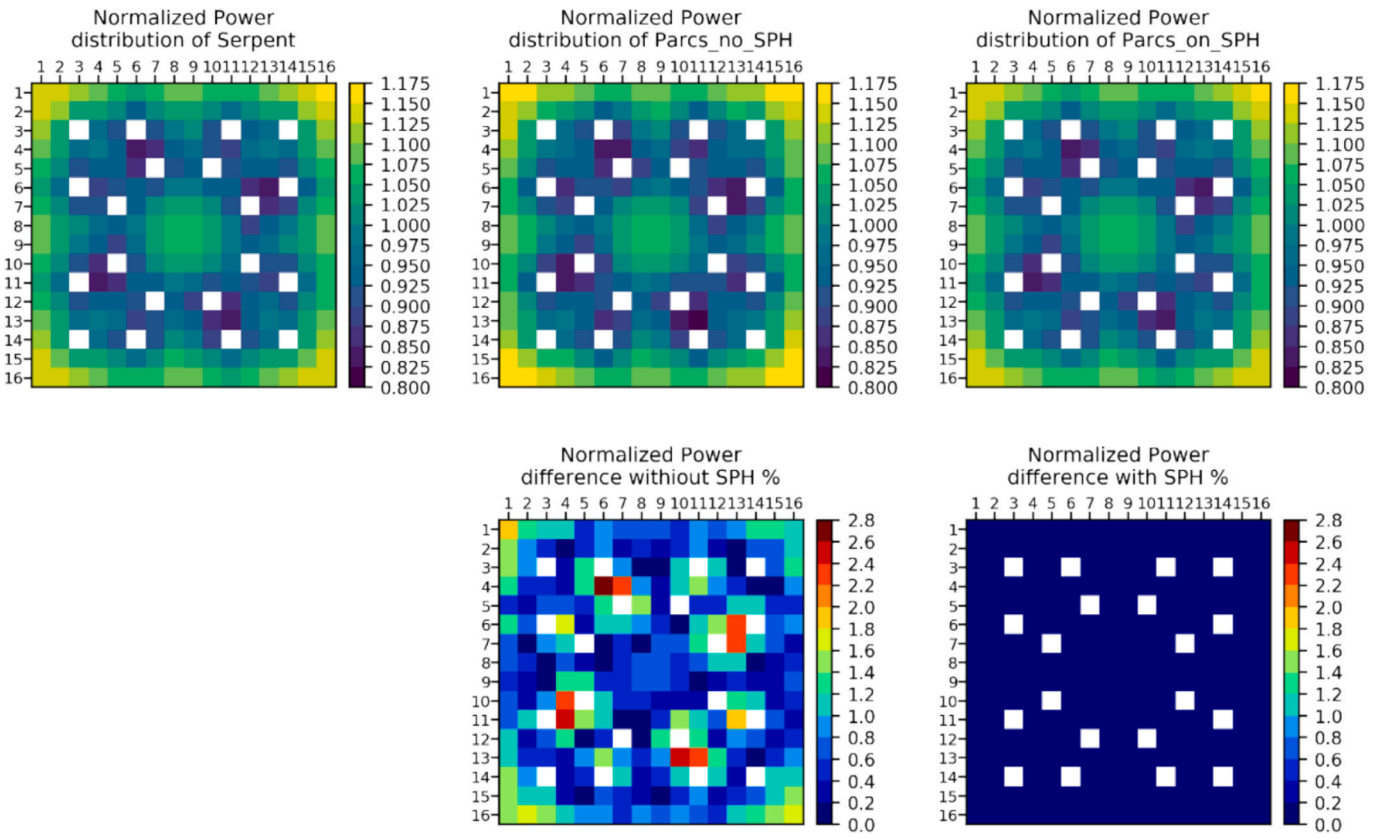

Fig. 12. The normalized pin power distribution of the KONVOI type assembly subcase 9.

Table 4
The maximum relative power difference between PARCS and Serpent2 of the KONVOI type assemblies.

	no SPH	on SPH
subcase 1	0.450 %	0.0207 %
subcase 2	0.413 %	0.0247 %
subcase 3	0.648 %	0.0301 %
subcase 4	0.820 %	0.0203 %
subcase 5	0.739 %	0.0289 %
subcase 6	0.707 %	0.0294 %
subcase 7	3.24 %	0.0254 %
subcase 8	3.04 %	0.0317 %
subcase 9	2.61 %	0.0394 %

considerable positive effect on predicting the pin power.

4.4. The KSMR core

KSMR core is an academic SMR core developed at KIT, based on the SMART reactor (Alzaben et al., 2019). It consists of 57 fuel assemblies across six types, with radially and axially varying enrichment levels ranging from 2.0 to 4.0 %. The fuel assemblies are arranged in a 17x17 rod configuration and feature 24 guide tubes and a central instrument tube, similar to typical Pressurized Water Reactor (PWR) assemblies. Since the KSMR is a boron-free core, each assembly contains 20 or 24 burnable poison rods with absorbers made of Al_2O_3 mixed with B_4C. The radial and axial layouts of the core and fuel assemblies are shown in Fig. 15.

Fifty-three of the fuel assemblies are equipped with control rods, divided into two banks: the regulating bank and the safety shutdown bank. The regulating bank includes 16 Ag-In-Cd control rods for coarse reactivity control and 17 hybrid rods made of Ag-In-Cd and stainless steel for fine control. The safety shutdown bank consists of 20 B_4C rods

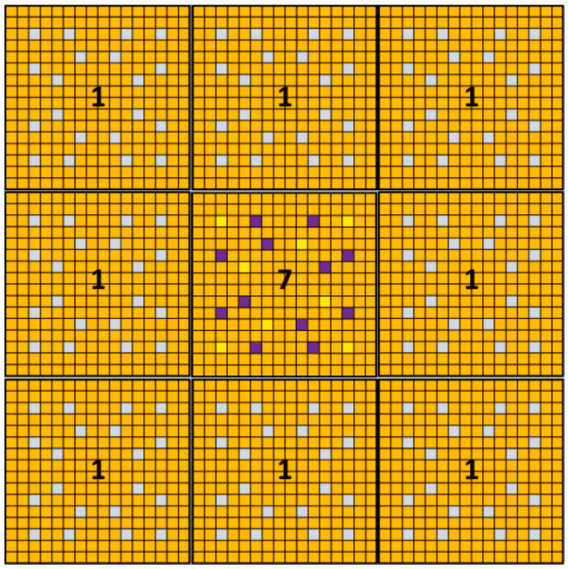

Fig. 13. The configuration and the geometrical dimension of the 3x3 mini assembly.

Table 5
The Keff results of the 3x3 mini core.

	Serpent2	PARCS tradition	PARCS no SPH	PARCS on SPH
Keff	1.18176	1.17900	1.18048	1.18068
K-Diff (PARCS-Serpent2) *10E5		−276	−128	−108

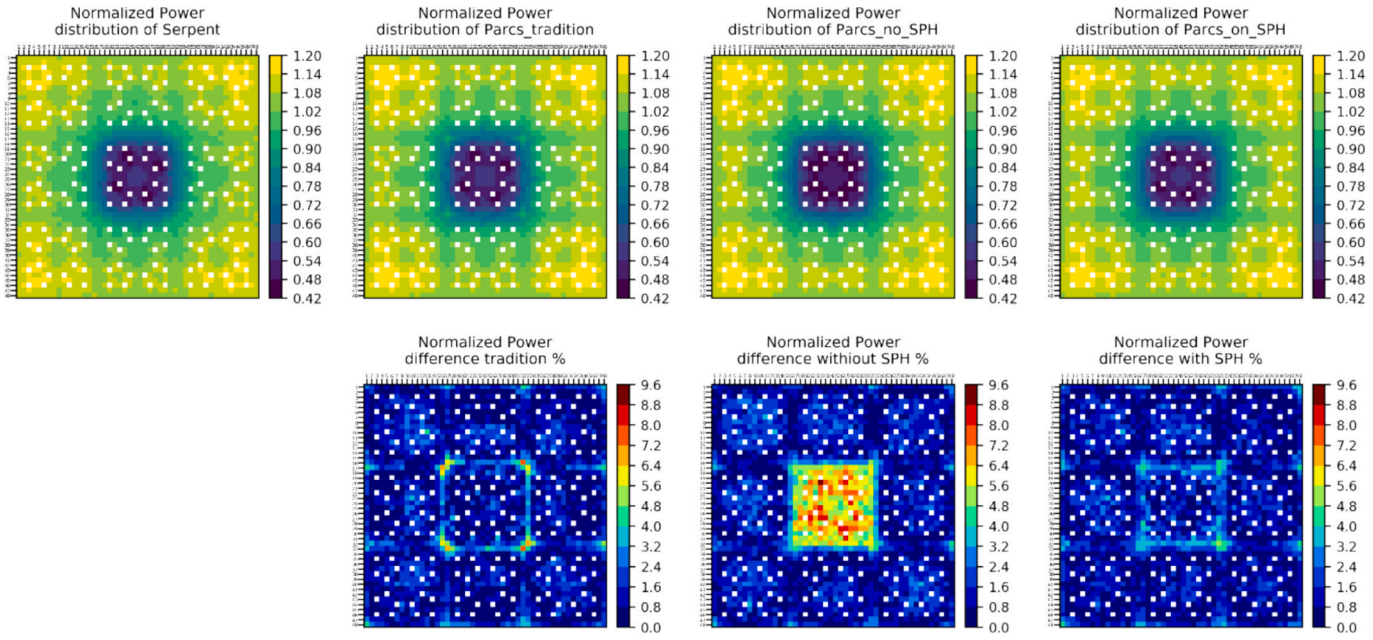

Fig. 14. The normalized pin power distribution of the 3x3 mini core.

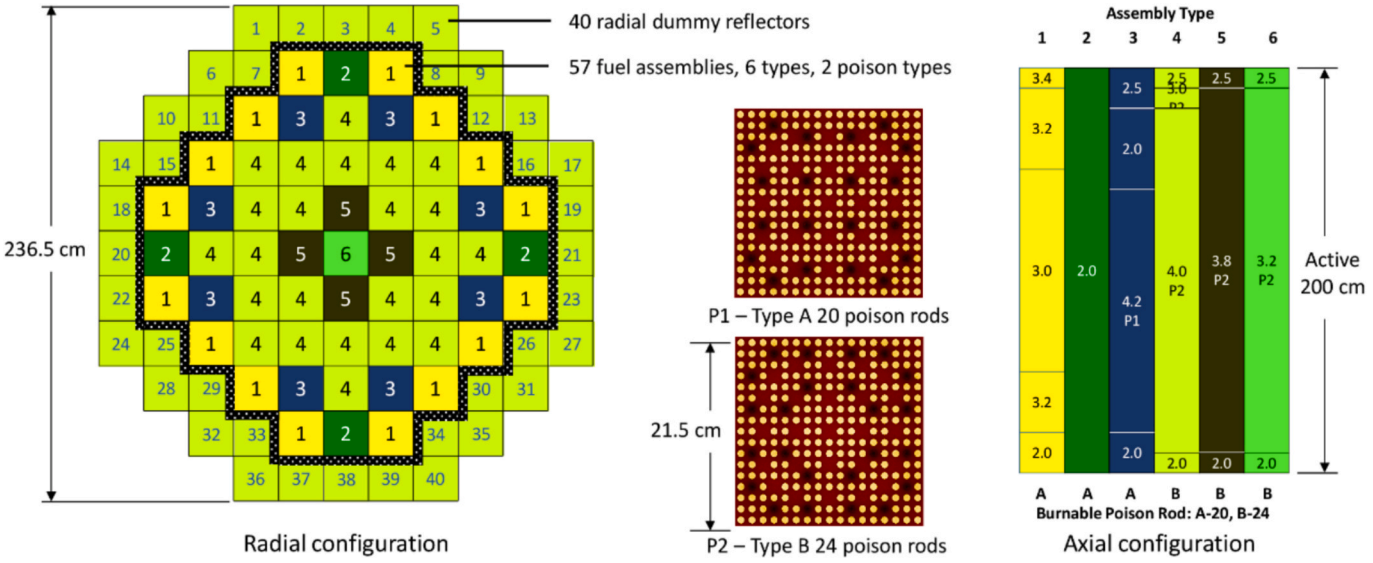

Fig. 15. The radial and axial layout of the fuel assemblies of the KSMR core.

that are fully withdrawn during normal operation. The radial and axial layouts of these control rods are illustrated in Fig. 16.

The variation in fuel enrichment, control rods, and burnable poison configurations leads to 35 distinct material configurations. For each configuration, multiple branches are processed by the XS correction system to generate the XS database for KSMR. Thus, the total number of cases processed amounts to 35 multiplied by the number of branches. The workflow for this system is as follows:

1) The system generates the necessary input files for both Serpent2 and PARCS.
2) Serpent2 runs multiple times to produce files containing pin-wise XS.
3) Input files for GenPMAXS are created, and along with the files from step 2, they are processed by GenPMAXS to generate raw XS for PARCS.
4) For each case, PARCS runs multiple iterations, reading iteratively updated XS until the power field difference with Serpent2 meets a set criterion.
5) Once all cases are completed, the final SPH-corrected pin-wise XS for all configurations are generated.

The overall workflow of the correction system for this case is presented in Fig. 17. With these corrected pin-wise XS, PARCS can simulate the full core under a wide range of operating conditions. It is to noting that the fuel XS is produced by a series of assembly-level simulations by Serpent, then corrected by the SPH system. The reflector XS (including the radial and axial reflectors) is produced from the whole core simulation of Serpent (dummy reflectors treated as water) and is not corrected due to its boundary nature.

In this paper, we focus on the hot zero power (1.0e-6 of nominal power) All Rod Out (ARO) condition. In addition to the SPH-corrected simulation, two other cases are included for comparison: a) without

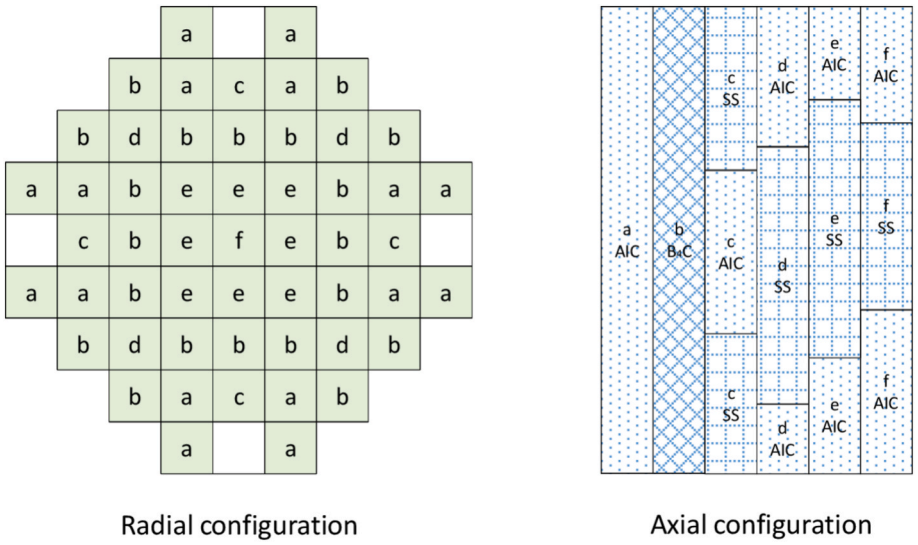

Fig. 16. The radial and axial layout of the control rods of the KSMR core (AIC – AgInCd, SS – Stainless Steel).

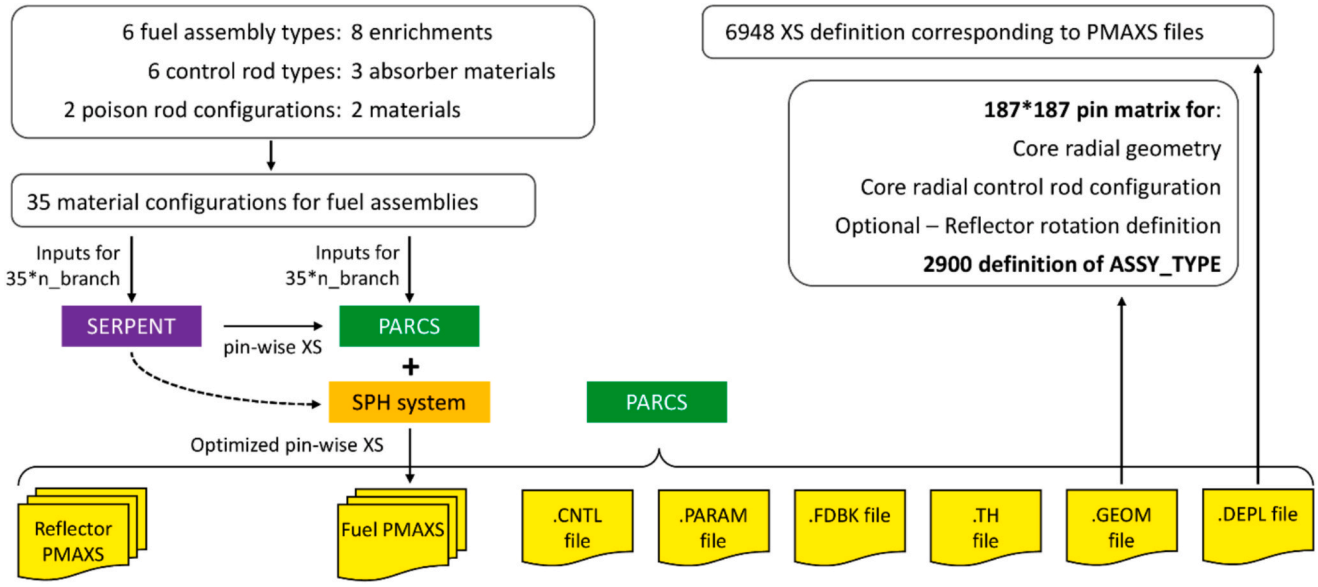

Fig. 17. The running procedures of the correction system for the verification with the KSMR core.

SPH correction, and b) the traditional assembly-wise solution with PPR. The without-SPH pin-level simulation is done with the raw fuel and reflector XS from Serpent. The assembly or nodal simulation uses the nodal-homogenized XS generated from Serpent. It is to noting that the nodal simulation applies the radial and axial discontinuity factors, while the pin-level simulations focus on verifying the effectiveness of the SPH system and do not include those factors at the moment. Nevertheless, future studies could take this into account.

Table 6 presents the Keff calculated by the three PARCS simulations along with the Serpent solution as the reference. It can be seen that the traditional nodal solution of PARCS gives the best result. The PARCS pin-level simulation without SPH correction produces a deviation as large as 0.01949, which is unacceptable. Whereas the deviation is significantly reduced to 0.00116 when the pin-level XS is corrected by the SPH system, proving the effectiveness of this system. As the difference is still non-negligible compared to the traditional nodal solution, application of pin discontinuity factors as well as the heterogeneous leakage models should be necessary to refine the on-SPH pin-level simulations in the future.

Table 6
The Keff results of the KSMR core.

	Serpent2	PARCS tradition	PARCS no SPH	PARCS on SPH
Keff	1.05373	1.05367	1.03424	1.05489
K-Diff (PARCS-Serpent2) *10E5		−6	−1949	116

The axial-integrated normalized power distributions for each case are shown in Fig. 18. The results indicate that the PPR and SPH-corrected solutions are closely aligned, while the solution without SPH shows a noticeable difference. To further illustrate, the three solutions are compared with the full-core Serpent2 solution, and the differences are calculated as (abs(PARCS-Serpent2)/Serpent2). The difference fields are depicted in Fig. 19, highlighting the poor prediction of the power field in the central and boundary regions for the No-SPH solution, while the other two methods perform well.

Note that the maximum difference in the color bar is 48 %, which is too large to effectively distinguish between the PPR and On-SPH

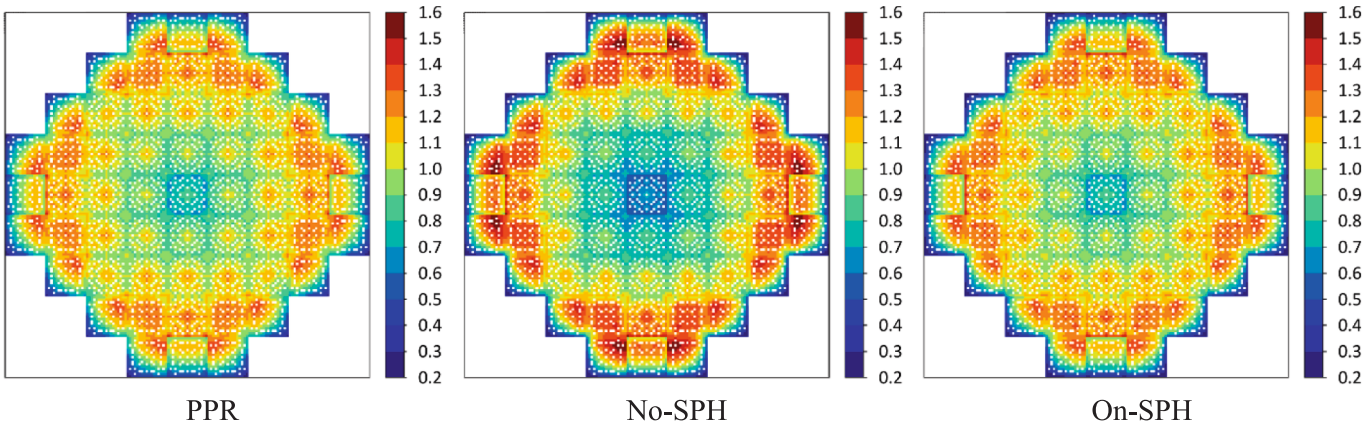

Fig. 18. The axial-integrated normalized power distributions by PARCS assembly-wise solution with PPR, pin-wise solution without SPH correction, and pin-wise solution with SPH correction.

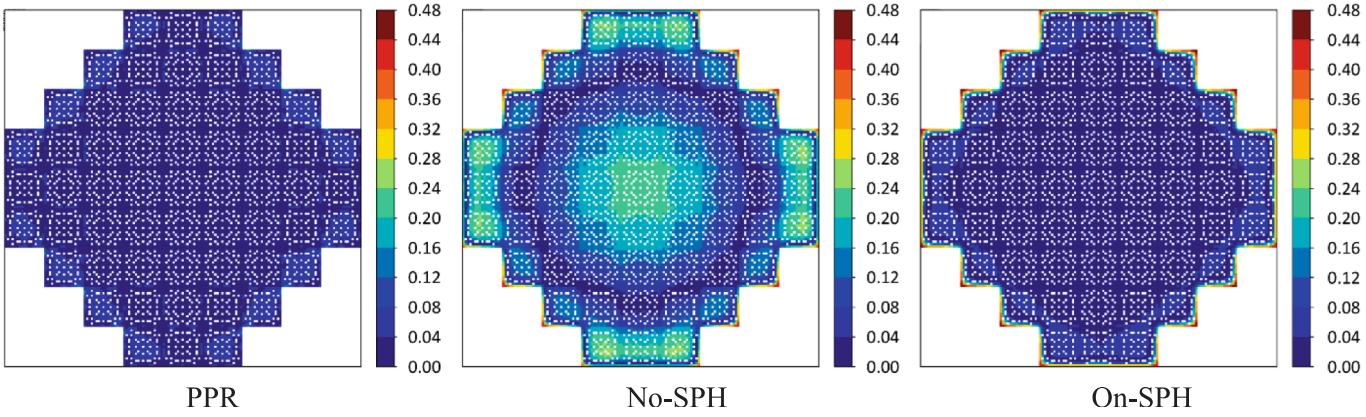

Fig. 19. The power differences between the Serpent2 solution and the PARCS assembly-wise solution with PPR, pin-wise solution without SPH correction, and pin-wise solution with SPH correction.

solutions. Consequently, we omit the No-SPH solution, set the maximum difference to 6 %, and re-scale the figure, resulting in Fig. 20. As shown in the figure, the On-SPH solution provides better predictions in most core areas, particularly in the central region, except for some boundary areas. The areas with better predictions are marked in green, while the areas with poorer predictions are indicated in red, as presented on the rightmost side of Fig. 20. The poor results observed at the boundaries are attributed to the modeling quality of the reflectors. Nonetheless, the correction system enhances simulation accuracy in most core areas, as anticipated.

Considering that the 2D axial-integrated radial normalized power is not sufficient to check the 3D spatial prediction between the solutions, we plot them in Fig. 21. Here, we observe that the spatial normalized power distributions for the PPR and On-SPH solutions are similar, while the No-SPH solution shows significant differences from the other two.

For a clearer understanding of the spatial differences among the three PARCS solutions compared to Serpent2, Fig. 22 illustrates the results. The No-SPH prediction demonstrates acceptable accuracy only within a narrow "band." Both PPR and On-SPH yield good spatial power predictions, though some differences remain. Notably, On-SPH

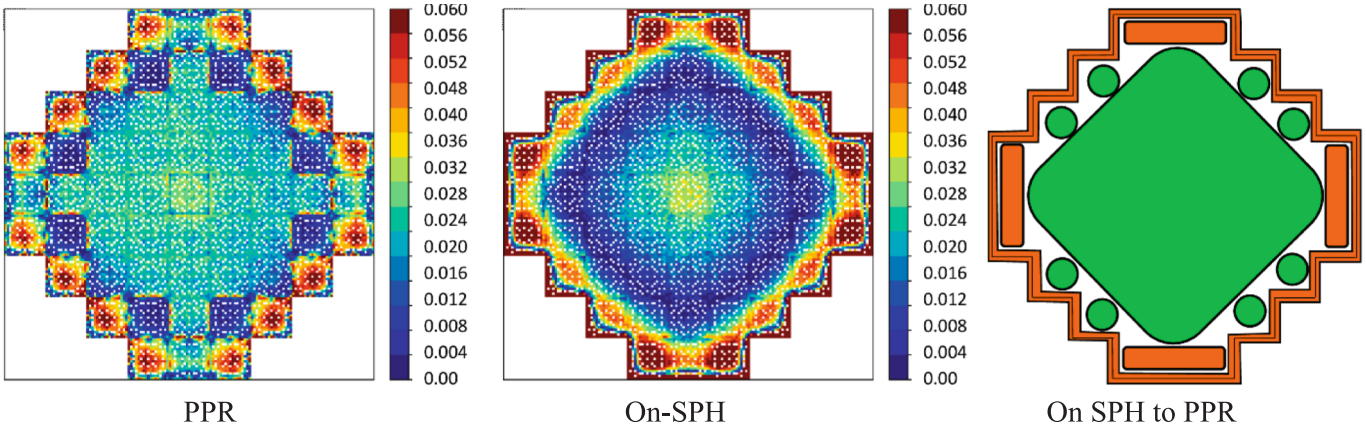

Fig. 20. The rescaled axial-integrated normalized power distributions by PARCS assembly-wise solution with PPR and pin-wise solution with SPH correction.

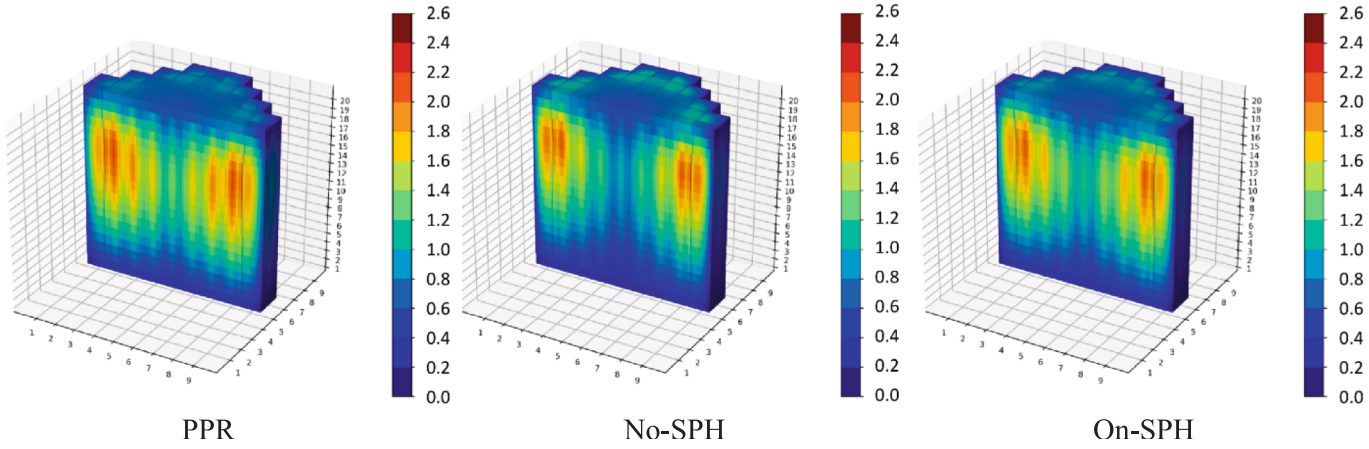

Fig. 21. The 3D spatial normalized power distributions by PARCS assembly-wise solution with PPR, pin-wise solution without SPH correction, and pin-wise solution with SPH correction.

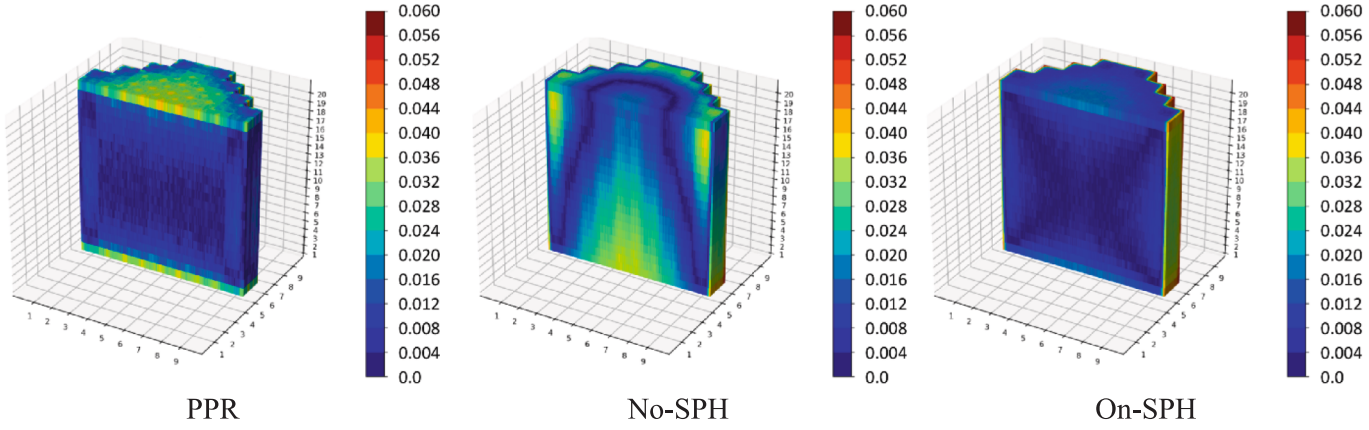

Fig. 22. The 3D power differences between the Serpent2 solution and the PARCS assembly-wise solution with PPR, pin-wise solution without SPH correction, and pin-wise solution with SPH correction.

significantly improves the power distribution at the upper and lower boundaries, although the results at the radial boundaries are poor. Additionally, the power distribution from On-SPH is much smoother than that from PPR, which is primarily due to the former being a true pin-wise simulation, whereas the latter represents an approximation that inherently contains "continuity errors.".

In summary, without SPH correction for pin-wise XS, PARCS cannot perform true pin-wise simulations or produce acceptable pin-wise results. With correction, PARCS can deliver high-quality pin-wise results, often surpassing those of traditional PPR simulations in most critical core areas. In terms of computational performance, the KSMR study required a total of 805 assembly-level branch cases to be simulated with Serpent2 to generate the reference XS. These Monte Carlo runs constituted the main computational effort. Once the Serpent data were available, the SPH correction loop was highly efficient: each PARCS run was fast, and convergence was typically achieved within 20–50 iterations per case. Owing to the automated Python framework, the SPH correction of all 805 cases was completed in about one hour on a standard workstation. This shows that the correction system itself introduces only modest computational overhead compared to the cost of reference XS generation.

At last, it is worth noting that the present verification study was restricted to a hot zero power condition. Although the SPH procedure is inherently independent of the absolute power level due to its use of normalized reaction rates, extending the validation to different operating powers and transient conditions would be of interest. Similarly, a more systematic exploration of partially inserted rod states would further enhance the assessment. Such an extension would require a large set of full-core Serpent simulations, which is computationally very demanding. Therefore, this task is deferred to future work.

5. Conclusions

In this work, a pin-wise cross-section (XS) correction system based on the SuPer-Homogenisation (SPH) method has been developed and implemented in a Python-based framework for use with PARCS. The system enables PARCS, originally designed for assembly-wise nodal simulations, to perform true pin-wise calculations with nodal solver and corrected homogenized XS. The methodology was verified through four cases of increasing complexity, ranging from a 3×3 mini assembly to the full core of the KIT Small Modular Reactor (KSMR). In all cases, the SPH correction significantly improved the agreement between PARCS and Serpent2 reference solutions in terms of keff and pin power distributions. Compared to the conventional Pin Power Reconstruction (PPR) approach, the SPH-corrected results provided more accurate predictions, particularly in central core regions, thereby demonstrating the feasibility of high-fidelity pin-wise simulations within the PARCS framework. The significance of this development lies in extending the capability of PARCS to support pin-resolved multi-physics analyses. By enabling accurate pin-wise neutronics, the corrected XS system provides a foundation for coupling PARCS with sub-channel thermal–hydraulic solvers, thereby allowing more reliable predictions of local safety

parameters under realistic operating conditions. This integration is expected to contribute to advanced reactor safety studies and to the assessment of innovative reactor concepts.

At the same time, certain limitations of the present work must be acknowledged. The treatment of reflector regions was simplified, leading to reduced accuracy at radial boundaries. In addition, the current validation was restricted to fresh fuel conditions, while burnup introduces additional XS variations that must be treated systematically. Both aspects can be addressed in future extensions, for example, by incorporating discontinuity factor corrections, improved SPH formulations at boundaries, and burnup-dependent XS libraries. Further validation under different power levels and control rod states will also be pursued to broaden the applicability of the method.

In summary, the developed SPH-based XS correction system represents a practical and effective approach to enhance the fidelity of PARCS pin-wise simulations. With the planned extensions, the methodology has strong potential to become a comprehensive tool for full-core high-resolution reactor multi-physics analyses and advanced safety evaluations.

CRediT authorship contribution statement

Kanglong Zhang: Writing – original draft, Software, Resources, Methodology, Formal analysis. **Luigi Mercatali:** Writing – review & editing. **Victor Hugo Sanchez-Espinoza:** Funding acquisition, Conceptualization.

Declaration of competing interest

The authors declare that they have no known competing financial interests or personal relationships that could have appeared to influence the work reported in this paper.

Acknowledgments

This work has received funding from the Euratom research and training program 2019–2020 under grant agreement No 945063 H2020 McSAFER project and the NUSAFE program of the Karlsruhe Institute of Technology (KIT).

Data availability

The authors do not have permission to share data.

References

Alzaben, Y., Sanchez-Espinoza, V.H., Stieglitz, R., 2019. Core neutronics and safety characteristics of a boron-free core for Small Modular Reactors. Ann. Nucl. Energy 132, 70–81. https://doi.org/10.1016/j.anucene.2019.04.017.

Zhuang, K., Wang, Y., Yan, J., Zou, H., Deng, L., Wang, Y., Wang, S., Zhang, Q., Zhang, J., 2024. Research on pin-by-pin calculation method of rectangular mesh based on quasi-diffusion theory. Ann. Nucl. Energy 205. https://doi.org/10.1016/j.anucene.2024.110584.

T. Downar, Y. Xu, and V. Seker, Theory Manual for the PARCS Kinetics Core Simulator Module, 2012.

Grundmann, U., Mittag, S., 2011. Super-homogenisation factors in pinwise calculations by the reactor dynamics code DYN3D. Ann. Nucl. Energy 38 (10), 2111–2119. https://doi.org/10.1016/j.anucene.2011.06.030.

Hebert, A., 1993. Consistent technique for the pin-by-pin homogenization of a pressurized water reactor assembly. Nucl. Sci. Eng. 113 (3), 227–238. https://doi.org/10.13182/NSE92-10.

A. Hébert and A. Kavenoky, "Development of the SPH homogenization method," in: International topical meeting on advances in mathematical methods for nuclear engineering problems, Munich, Germany, (1981).

Hébert, A., Benoist, P., 1991. A consistent technique for the global homogenization of a pressurized water reactor assembly. Nucl. Sci. Eng. 109 (4), 360–372. https://doi.org/10.13182/NSE109-360.

Hebert, A., Mathonniere, G., 1993. Development of a third-generation superhomogeneization method for the homogenization of a pressurized water reactor assembly. Nucl. Sci. Eng. 115 (2), 129–141. https://doi.org/10.13182/NSE115-129.

A. Kavenoky, The SPH homogenization method (IAEA-TECDOC–231), 1980.

Kim, W., Heo, W., Kim, Y., 2017. Improvement of nodal accuracy by using albedo-corrected parameterized equivalence constants. Nucl. Sci. Eng. 188 (3), 207–245. https://doi.org/10.1080/00295639.2017.1354592.

Kim, J., Kim, Y., 2019. Development of 3-D HCMFD algorithm for efficient pin-by-pin reactor analysis. Ann. Nucl. Energy 127, 87–98. https://doi.org/10.1016/j.anucene.2018.11.035.

Kim, J., Kim, Y., 2020. Three-dimensional pin-resolved transient diffusion analysis of PWR core by the hybrid coarse-mesh finite difference algorithm. Nucl. Sci. Eng. 194 (1), 1–13. https://doi.org/10.1080/00295639.2019.1642016.

E. Lemarchand, M. Klein, I. Pasichnyk, K. Velkov, and W. Zwermann, Pin-by-Pin Calculations with QUABOX/CUBBOX using the Super Homogenization Method, Garching, Germany.

Labouré, V., Wang, Y., Ortensi, J., Schunert, S., Gleicher, F., DeHart, M., Martineau, R., 2019. Hybrid super homogenization and discontinuity factor method for continuous finite element diffusion. Ann. Nucl. Energy 128, 443–454. https://doi.org/10.1016/j.anucene.2019.01.003.

Leppänen, J., Pusa, M., Viitanen, T., Valtavirta, V., Kaltiaisenaho, T., 2015. The Serpent Monte Carlo code: status, development and applications in 2013. Ann. Nucl. Energy 82, 142–150. https://doi.org/10.1016/j.anucene.2014.08.024.

Li, X., Liu, X., Chai, X., He, H., Zhang, B., Zhang, T., 2023. Multi-physics coupling simulation of small mobile nuclear reactor with finite element-based models. Comput. Phys. Commun. 293, 108900. https://doi.org/10.1016/j.cpc.2023.108900.

Nikitin, E., Fridman, E., Mikityuk, K., 2015. On the use of the SPH method in nodal diffusion analyses of SFR cores. Ann. Nucl. Energy 85, 544–551. https://doi.org/10.1016/j.anucene.2015.06.007.

Ortensi, J., Wang, Y., Laurier, A., Schunert, S., Hébert, A., DeHart, M., 2018. A Newton solution for the Superhomogenization method: the PJFNK-SPH. Ann. Nucl. Energy 111, 579–594. https://doi.org/10.1016/j.anucene.2017.09.027.

Sen, R.S., Hummel, A.J., Hiruta, H., 2017. Super-homogenization-corrected cross-section generation for high-temperature reactors. Idaho.

Smith, K.S., 1986. Assembly homogenization techniques for light water reactor analysis. Prog. Nucl. Energy 17 (3), 303–335. https://doi.org/10.1016/0149-1970(86)90035-1.

A. Ward, Y. Xu, and T. Downar, Code for Generating the PARCS Cross Section Interface File PMAX, 2016.

Wang, X., Zhuang, K., Qiu, Z., Wang, L., Lu, D., Zhang, B., Wang, S., 2025. Research on reactor core pin-by-pin calculation based on new leakage corrected SPH method. Ann. Nucl. Energy 213. https://doi.org/10.1016/j.anucene.2024.111150.

Yamamoto, A., Tatsumi, M., Kitamura, Y., Yamane, Y., 2004. Improvement of the SPH method for pin-by-pin core calculations. J. Nucl. Sci. Technol. 41 (12), 1155–1165.

Y. Yuan, G. Liu, and X. Huo, "Implementation and Comparison of Super Homogenization Method Based on Monte Carlo and Deterministic Codes," in 2022 29th International Conference on Nuclear Engineering, Virtual online, 2022.

Zhang, B., Li, Y., Wu, H., Zhao, W., Fang, C., Gong, Z., Li, Q., Chai, X., Yu, J., 2024. PWR core calculation based on pin-cell homogenization in three-dimensional pin-by-pin geometry. Nucl. Eng. Technol. 56 (6), 1950–1958. https://doi.org/10.1016/j.net.2024.01.002.